ASTRONOMY & ASTROPHYSICS
SUPPLEMENT SERIES

JANUARY II **1998**, PAGE 277

Astron. Astrophys. Suppl. Ser. **127,** 277-294 (1998)

Are metallic A-F giants evolved Am stars? Rotation and rate of binaries among giant F stars⋆,⋆⋆

M. Künzli and P. North

Institut d'Astronomie de l'Université de Lausanne, CH-1290 Chavannes-des-Bois, Switzerland

Received October 30, 1996; accepted May 9, 1997

Abstract. We test the hypothesis of Berthet (1992) which foresees that Am stars become giant metallic A and F stars (defined by an enhanced value of the blanketing parameter Δm_2 of the Geneva photometry) when they evolve.

If this hypothesis is right, Am and metallic A-FIII stars need to have the same rate of binaries and a similar distribution of $v \sin i$. From our new spectroscopic data and from $v \sin i$ and radial velocities in the literature, we show that it is not the case. The metallic giant stars are often fast rotators with $v \sin i$ larger than 100 $\mathrm{km\,s^{-1}}$, while the maximum rotational velocity for Am stars is about 100 $\mathrm{km\,s^{-1}}$. The rate of tight binaries with periods less than 1000 days is less than 30% among metallic giants, which is incompatible with the value of 75% for Am stars (Abt & Levy 1985). Therefore, the simplest way to explain the existence of giant metallic F stars is to suggest that all normal A and early F stars might go through a short "metallic" phase when they are finishing their life on the main sequence.

Besides, it is shown that only giant stars with spectral type comprised between F0 and F6 may have a really enhanced Δm_2 value, while all A-type giants seem to be normal.

Key words: stars: binaries: spectroscopic — stars: chemically peculiar — stars: evolution — stars: rotation — stars: δ Scuti

1. Introduction

Main sequence A and F stars show various interesting phenomena: chemical peculiarities (Am, Fm, Ap...) on the one hand and/or pulsation on the other hand. Numerous studies have been devoted to this part of the HR diagram near the ZAMS, but few have explored more evolved stars. In this paper, we examine the rate of binaries and rotation of giant A and F stars.

In a study of 132 giant A and F stars, Hauck (1986) showed that 36% of them have an enhanced value of the blanketing parameter Δm_2 (defined roughly speaking by $m_2(\mathrm{observed}) - m_2(\mathrm{Hyades})$) characterising Am and δ Del stars. He showed also that this parameter could probably be interpreted in terms of metallicity for giant A and F stars. This interpretation was confirmed by Berthet (1990, 1991) from a detailed abundance analysis of such objects. His study pointed out that these stars have chemical properties similar to those of δ Del stars, i.e. an overabundance of iron peak elements and especially of heavier elements such as Sr and Ba, and solar composition for Ca and Sc. Am stars have similar characteristics for iron peak elements, but Ca and Sc are deficient by factors of about 10.

Based on chemical abundances, position in the (β, M_v) plane of Strömgren photometry, rotation and duplicity of δ Del stars, Kurtz (1976) suggested that these stars are evolved Am stars. The fact that δ Del and giant metallic A and F stars harbour similar chemical properties suggests also a link between Am and giant metallic A and F stars. Thus, a star could begin its life on the main sequence as an Am star, then, as abundances of Ca and Sc increase to quasi-solar values with evolution, it would become a δ Del star and finally a giant metallic A-F where Ca and Sc are solar (Berthet 1992).

To explain the emergence of chemical anomalies in Am stars, one generally invokes the radiative diffusion theory developed by Michaud et al. (1983). This theory predicts that, in slow rotators, helium is no longer sustained and flows inside the star and gradually disappears from the atmosphere. The diffusion process could therefore take place just below the thin H convective zone where the diffusion time is short with respect to the stellar lifetime; the chemical elements whose radiative acceleration is larger than gravity become overabundant and, in the opposite

Send offprint requests to: P. North

⋆ Based on observations collected at Observatoire de Haute Provence (OHP), France.

⋆⋆ Tables 2, 3, 6 are also available in electronic form at CDS via anonymous ftp to cdsarc.u-strasbg.fr (130.79.128.5) or via http://cdsweb.u-strasbg.fr/Abstract.html

case, underabundant. The convective zone becomes deeper with evolution and so leads to normalisation of the surface abundance. This theory explains the chemical anomalies in Am stars and the increase of Ca and Sc abundances with time.

The chemical anomalies predicted by the diffusion theory are generally larger than the observed anomalies. These differences come from uncertainties of the atomic data but also from some mechanism in the stellar atmosphere. The mass loss probably takes a prominent part: a rate of about 10^{-15} $M_\odot$/year is sufficient to reduce the theoretical overabundance of heavy elements to observed abundances (Charbonneau & Michaud 1991). Fast rotation ($v \sin i > 120$ km s^{-1}) generates meridional circulation which prevents the disappearance of the helium ionisation zone, so the metallic anomalies cannot appear (Michaud 1983). Observationally, the upper limit of rotation for Am stars is about 100 km s^{-1} (Abt & Moyd 1973), while for normal stars, we observe projected rotational velocities larger than 100 km s^{-1}, which is in agreement with the diffusion theory. The meridional circulation cannot be invoked to reduce theoretical abundances to observed ones: in some cases, they can increase the theoretical abundances and qualitatively no relation exists between $v \sin i$ and the chemical anomalies in the velocity range characteristic of Am and Fm stars ($0-100$ km s^{-1}). Indeed, the time diffusion under the hydrogen convective zone is shorter than that of the meridional circulation.

The rate of binaries is completely different in Am and normal stars: Am stars are often members of tight binaries ($P \leq 100$ days), while normal stars in double systems often have larger periods ($P > 100$ days). So, we would be tempted to explain the low rotation of Am stars by tidal braking. Nevertheless, Zahn (1977) showed that this effect is really important only for tight binaries with a period less than 7 days. On the other hand, Abt & Levy (1985) showed that 75% of Am stars have periods below 1000 days, so they do not necessarily belong to tight binaries. Other mechanisms must contribute to reduce the rotational velocity to 100 km s^{-1} or less. One of them may be the evolutionary expansion of stars during their main sequence lifetime. According to Abt & Levy (1985), during this phase, the velocity decreases by a factor of 2 and consequently most of the normal A stars may become Am stars before leaving the main sequence. These authors suggest also the possibility of tidal braking during the pre-main sequence phase to explain the exclusion of normal stars with a period comprised between 10 and 100 days.

The goal of the present work is to compare the $v \sin i$ and the rate of binaries among Am and giant metallic A and F stars in order to consider the possibility of a link between these two types of stars. To this end, we have measured at OHP some of Hauck's stars having no radial velocities or $v \sin i$, or only old determinations. These data should allow to strengthen a preliminary work (North 1994) which casts some doubts on the validity of the scenario advocated by Berthet (1992).

2. The sample and the observations

We defined the sample to be observed from Table 3 and Table 4 of Hauck (1986). The reason why we considered Table 4 (containing stars classified spectroscopically as dwarfs but photometrically as giants) was that the photometric criterion of luminosity seems much more reliable than the spectroscopic luminosity class.

The selection criteria were:

- Visibility from OHP ($\delta \gtrsim -20°$)
- Insufficient V_r data or unknown $v \sin i$.

By insufficient V_r, we mean that the star has less than three published V_r values in the literature. Applying these criteria, 50 A and F giant stars were selected, both normal and metallic. It was judged useful to have a good estimate of the binary freqency of normal A and F giants for reference purposes. 40 stars in the sample are non-metallic, while only ten are metallic according to the criterion $\Delta m_2 \geq 0.013$ (see Sect. 5.1). Thus, the estimate of binary frequency among metallic giants will mainly rely upon old, published V_r data. The Δm_2 values of the sample stars range between -0.027 and 0.082. They have been updated using a new reference sequence in the $m_2/B2-V1$ diagram (Hauck et al. 1991), and sometimes by complementary photometric measurements. Eight stars belong to the δ Scuti class, and nine are spectroscopically classified as dwarf but have a large Δd parameter (Δd is the luminosity parameter of Geneva photometry, equivalent to Strömgren's δc_1) indicating that they very probably are real giants. All stars are bright, with $V \leq 7.0$, implying that interstellar reddening is insignificant.

The observations were performed at the Observatoire de Haute Provence (OHP) with the Aurélie spectrograph attached to the 1.52 m telescope at the Coudé focus (Gillet et al. 1994) in 1994. Four runs of a few nights' duration each were made respectively at the beginning of May and June for 18 stars and at the beginning of November and December for 32 stars. These measurements should allow to detect binary stars with a small period ($P \lesssim 100$ days).

The detector is a double barrette CCD Thomson TH7832 with 2048 pixels having a size of 750×13 μm. The spectra were obtained at a reciprocal dispersion of 8 Å mm^{-1} in the spectral region centred on Hβ [4780 Å, 5000 Å]. The reduction was made at the OHP with IHAP procedures, using comparison spectra of thorium. Each stellar measurement was preceded by a calibration exposure to compensate for instrumental drift as much as possible. To normalise our spectrum, we simply fit a straight line to the continuum. 291 stellar exposures were made, of which 54 were devoted to standard stars. For most of the spectra a signal-to-noise of 150 was achieved. The minimum number of exposures per star was 2 and the

maximum 11, with a mean value of 5 or 6 measurements per star.

3. Radial velocity determinations

3.1. Hβ fitted by a lorentz profile

Some stars of the sample rotate very fast and some are very hot, with effective temperature of about 8000 K. Therefore, these stars cannot be measured with an instrument such as Coravel, which needs many narrow lines. The adopted technique consists in fitting a lorentz profile on the Hβ line [4861.331 Å] minimising the χ^2, i.e. the differences between the lorentz profile and the observed line. The advantage of a lorentz function over a gaussian is to be more peaked at the centre, so hydrogen lines are better fitted.

A lorentz profile is defined by 3 parameters (Eq. 1): λ_0 is the centre, i_0 the intensity or height and b the half-intensity width of the profile.

$$L(\lambda) = \frac{i_0 b^2}{(\lambda - \lambda_0)^2 + b^2}. \quad (1)$$

The three parameters of $L(\lambda)$ are fitted by least-squares; meanwhile the optimum choice will depend on the limits fixing the spectral range on which the fit is made. To avoid too subjective a choice, we fix on both sides of the line two points determining a segment on which the limit is randomly chosen (Fig. 1). Thus, we generate 100 lorentz profiles with different limits on each Hβ line. A profile is taken into account only if the χ^2 value does not exceed 0.05 in order to avoid hazardous fits. Then, we define for each line Hβ the mean value of the central wavelength and the dispersion:

$$\overline{\lambda_0(\mathrm{H}\beta)} = \frac{1}{n}\sum_{i=i}^{n} \lambda_0(\mathrm{H}\beta)_i, n = 100 \quad (2)$$

$$\sigma_{\lambda_0(\mathrm{H}\beta)} = \sqrt{\sum_{i=i}^{n} \frac{1}{n}(\lambda_0(\mathrm{H}\beta)_i - \overline{\lambda_0(\mathrm{H}\beta)})^2}, n = 100. \quad (3)$$

The dispersion $\sigma_{\lambda_0(\mathrm{H}\beta)}$ depends on the physical properties of the star, essentially the temperature, the surface gravity and the rotation but also the quality of the spectrum, i.e. the signal-to-noise. We have chosen to distribute the V_r measurements into categories of decreasing discrete precision on the basis of $\sigma_{\lambda_0(\mathrm{H}\beta)}$ values (see Table 1): measurements with $\sigma_{\lambda_0(\mathrm{H}\beta)}$ between 0 and 3 mÅ will be considered as having $\sigma^{\mathrm{s}}_{V_\mathrm{r}} = 0.19\ \mathrm{km\,s^{-1}}$, those with $\sigma_{\lambda_0(\mathrm{H}\beta)}$ between 3 and 6 mÅ will have $\sigma^{\mathrm{s}}_{V_\mathrm{r}} = 0.38\ \mathrm{km\,s^{-1}}$, etc. The value of 3 mÅ is completely arbitrary, corresponding to a radial velocity of about 0.2 $\mathrm{km\,s^{-1}}$. The $\sigma_{\lambda_0(\mathrm{H}\beta)}$ and the central wavelength $\overline{\lambda_0(\mathrm{H}\beta)}$ also depend on the choice of the limits for the fit. This effect is discussed in detail in Appendix A.

Table 1. Dispersion in radial velocity $\sigma^{\mathrm{s}}_{V_\mathrm{r}}$ from the dispersion in wavelength $\sigma_{\lambda_0(\mathrm{H}\beta)}$

$\sigma_{\lambda_0(\mathrm{H}\beta)}$ [Å]	$\sigma^{\mathrm{s}}_{V_\mathrm{r}}$ [$\mathrm{km\,s^{-1}}$]
[0.000, 0.003]	0.19
[0.003, 0.006]	0.38
[0.006, 0.009]	0.56
[0.009, 0.012]	0.74
...	

The term $\sigma^{\mathrm{s}}_{V_\mathrm{r}}$ is defined as the internal error due to the effective temperature, the surface gravity, the rotation and the S/N ratio. The total internal error includes an additional term due to the instrumental drift during the night. This variability was similar for the four missions and Figs. 2 and 3 show the fluctuations of the position of the thorium lines during the night of 6 and 7 November and during the night of 5 and 6 December 1994 for 3 lines. When we filled up the nitrogen tank, at the beginning and in the middle of the night, a strong variation appeared as shown on these figures. Between these jumps, we observe a regular variation of about 0.12 pixels per hour. We therefore have a variation of 0.16 $\mathrm{km\,s^{-1}}$ per 12 minutes which corresponds to the average time of stellar exposure. For this reason, the internal error due to this factor ($\sigma^{\mathrm{t}}_{V_\mathrm{r}}$) is estimated at 0.16 $\mathrm{km\,s^{-1}}$. Finally, the total internal error is written by $I = \sqrt{(\sigma^{\mathrm{s}}_{V_\mathrm{r}})^2 + (\sigma^{\mathrm{t}}_{V_\mathrm{r}})^2}$.

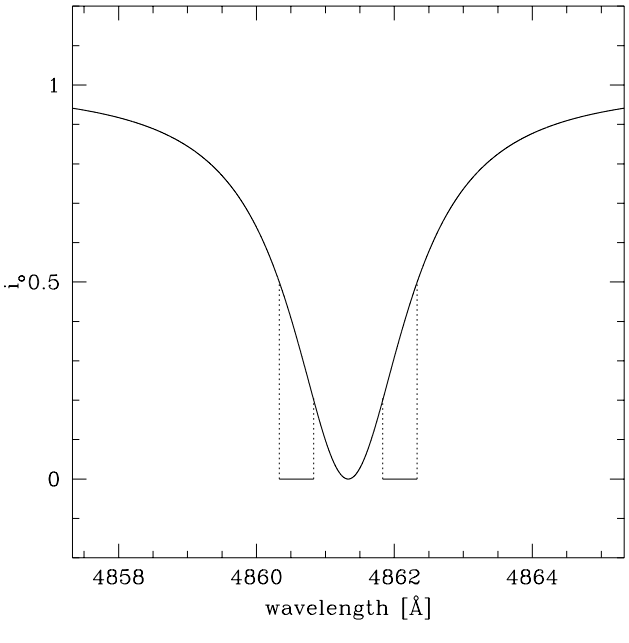

Fig. 1. The limits fixing the spectral range on which the fit is made are randomly chosen on two segments symmetrically placed with respect to the centre of the line

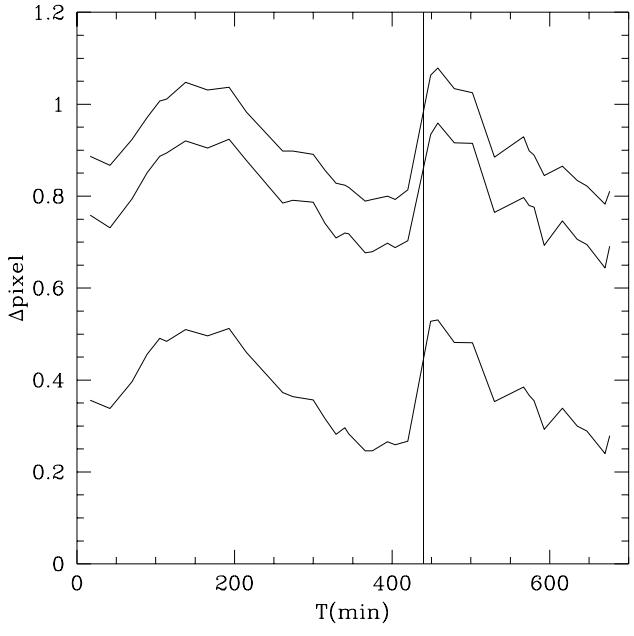

Fig. 2. Variation of the position of three lines of thorium during 6 and 7 November 1994. The vertical shift is arbitrary. The vertical line corresponds to the filling of nitrogen

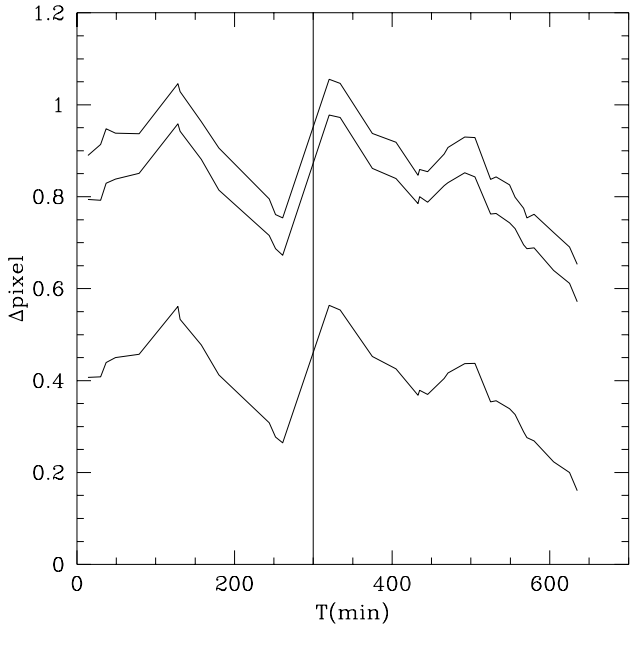

Fig. 3. Same as Fig. 2, but for the night of 5 and 6 December 1994

3.2. Standard stars

For standard stars, we prefer to use Coravel values in the system of faint IAU standard stars (Mayor & Maurice 1985) than IAU values listed in the Astronomical Almanach because the latter are taken from various authors and sometimes not updated. For example, the IAU radial velocity for HD 114762 has been listed as 49.9 ± 0.5 km s^{-1} in the Astronomical Almanach since at least 1981, while combined data from the Cfa and Coravel give a systemic velocity of 49.35 ± 0.04 km s^{-1} (Latham et al. 1989).

For the four observing runs, Fig. 4 shows the difference between radial velocities measured with Aurélie and the Coravel value for each standard star. Our values are higher than the Coravel ones by about 2.75 km s^{-1}. The error bars are defined by the quadratic sum of the internal error (see Sect. 3.1) and the dispersion on the Coravel values. The internal precision of our measurements is very impressive: we obtain a scatter of about 0.4 km s^{-1} around the mean radial velocity.

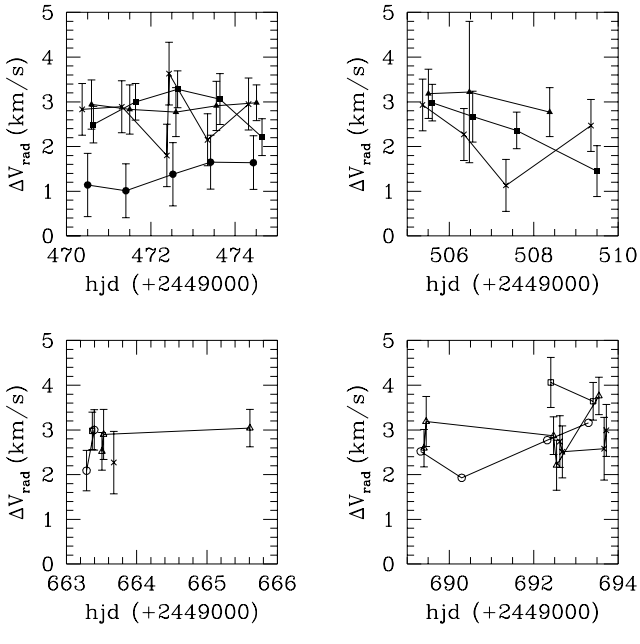

Fig. 4. Difference between Aurélie radial velocities and Coravel velocities for the runs of May, June, November and December 1994. HD 693: open squares. HD 22484: open triangles. HD 89449: crosses. HD 114762: full circles. HD 136202: full triangles. HD 222368: open circles

Notice that ΔV_r is clearly smaller for HD 114762 by about 1.4 km s^{-1}. Such a difference can partly be due to the nature of this star, which has a very small amplitude (Latham et al. 1989 and Cochran et al. 1991) and to the fact that our measurements were made precisely when the radial velocity was minimum: in this way we can explain

a shift of about 0.6 km s^{-1} with respect to the other standard stars. Unfortunately, we do not find any explanation for the remaining shift of 0.8 km s^{-1}. The reduction of the spectra was made again with MIDAS software, only to find the same shift. So, we cannot question the reduction.

We have simply subtracted the mean ΔV_r from the measured velocities. The average ΔV_r are 2.80, 2.49, 2.69 and 2.90 km s^{-1} for the runs of May, June, November and December respectively. For the first run, the values of HD 114762 are not taken into account in the average value. Table 2 gives the individual corrected radial velocities and the mean velocity for standard stars; Table 3 lists the individual corrected radial velocities for the 50 giant A and F stars.

4. Binarity among the sample

4.1. Criterion of variability

To take into account the errors of measurements on the determination of the duplicity, we computed the χ^2 value for each star of the programme: $\chi^2 = (n-1)(\frac{E}{I})^2$ where n is the number of measurements, E the external error and I the internal error. We then used an F-test which gives the probability $P(\chi^2)$ that the variations of velocity are only due to the internal dispersion. A star will be considered as double or intrinsically variable if $P(\chi^2)$ is less than 0.01 (Duquennoy & Mayor 1991). Naturally, this test cannot say anything about the nature of the variability.

The distribution of $P(\chi^2)$ for non-variable stars should be flat from 0 to 1, while the variable stars should gather at the smallest values of $P(\chi^2)$. Therefore, this method allows to appreciate a posteriori the estimate of internal errors. Indeed, if these errors are underestimated, a gradient appears in the distribution of $P(\chi^2)$ in favour of small values, while if they are overestimated, a peak appears near 1, indicating an abnormally strong predominance of constant stars.

In our case, the internal error is estimated by the quadratic sum of a term which depends on the width of the Hβ line and the quality of the spectrum, and a second term related with the instrumental shift during the night. While the last term is rather well controlled, the first one is not well-known. Indeed, it strongly depends on the choice of the limits (see Sect. 3.2). The internal error can be written:

$$I = \sqrt{(\alpha\sigma^{\rm s}_{V_r})^2 + (\sigma^{\rm t}_{V_r})^2} \qquad (4)$$

where $\sigma^{\rm s}_{V_r}$ is the dispersion due to $T_{\rm eff}$, $v \sin i$ and S/N, $\sigma^{\rm t}_{V_r}$ is the dispersion due to instrumental drift and α is adjusted to obtain a flat distribution of $P(\chi^2)$ on the interval [0,1], except for the small values of course. α indicates the quality of the preliminary estimation of I. To determine α quantitatively, one uses the cumulative distribution of $P(\chi^2)$ which must approximate a straight line in the case of a flat distribution. For a given α, one can

Table 2. Radial velocities of standard stars

HD	HJD (+2449000)	$V_r^{\rm OHP}$ km s^{-1}	I km s^{-1}
693	663.367	15.12	0.28
693	692.408	15.99	0.48
693	693.411	15.57	0.28
	$\overline{V_r}$ =	15.44±0.36	
22484	663.507	27.59	0.28
22484	663.528	27.97	0.48
22484	665.610	28.11	0.28
22484	689.403	27.45	0.28
22484	689.450	28.05	0.48
22484	692.473	27.73	0.28
22484	692.544	27.07	0.48
22484	693.546	28.62	0.28
	$\overline{V_r}$ =	27.86±0.44	
89449	470.375	6.07	0.28
89449	471.311	6.13	0.28
89449	472.383	5.04	0.48
89449	472.433	6.87	0.69
89449	473.347	5.39	0.28
89449	474.319	6.19	0.28
89449	505.366	6.49	0.28
89449	506.346	5.83	0.28
89449	507.345	4.69	0.28
89449	509.356	6.03	0.28
89449	663.674	5.62	0.48
89449	692.618	5.88	0.28
89449	692.681	5.65	0.28
89449	693.668	5.72	0.48
89449	693.722	6.13	0.28
	$\overline{V_r}$ =	5.84±0.52	
114762	470.503	47.51	0.48
114762	471.411	47.38	0.28
114762	472.526	47.75	0.48
114762	473.420	48.02	0.28
114762	474.432	48.01	0.28
	$\overline{V_r}$ =	47.77±0.26	
136202	470.593	54.33	0.48
136202	471.499	54.22	0.48
136202	472.597	54.16	0.48
136202	473.555	54.30	0.48
136202	474.504	54.37	0.28
136202	505.503	54.89	0.48
136202	506.474	54.93	1.56
136202	508.381	54.48	0.48
	$\overline{V_r}$ =	54.39±0.27	
187691	470.642	−0.58	0.28
187691	471.638	−0.07	0.28
187691	472.638	0.21	0.28
187691	473.640	−0.01	0.48
187691	474.639	−0.86	0.28
187691	505.598	0.23	0.28
187691	506.558	−0.08	0.48
187691	507.599	−0.39	0.28
187691	509.501	−1.30	0.48
	$\overline{V_r}$ =	−0.27±0.49	
222368	663.287	4.76	0.28
222368	663.395	5.67	0.28
222368	689.321	4.98	0.48
222368	690.296	4.39	0.28
222368	692.320	5.23	0.28
222368	693.300	5.62	0.28
	$\overline{V_r}$ =	5.12±0.45	

Table 3. Radial velocities of A and F giants

HD	HJD (+2449000)	V_r km s^{-1}	I km s^{-1}
1671	663.445	10.53	0.48
1671	689.354	10.55	0.28
1671	693.444	10.34	0.48
2628	663.451	−10.86	0.28
2628	689.366	−10.67	1.12
2628	693.448	−10.40	0.28
4338	663.410	2.08	0.69
4338	689.381	−0.47	1.34
4338	693.470	5.84	0.94
6706	663.426	23.81	0.28
6706	692.487	23.57	0.69
10845	663.458	−13.97	0.48
10845	689.412	−13.67	0.90
11522	663.436	1.16	0.69
11522	693.514	1.99	1.34
12573	663.471	8.62	0.69
12573	692.522	7.38	0.90
17584	689.423	18.41	0.94
17584	663.481	18.60	0.90
17584	692.387	19.42	0.69
17918	663.491	17.21	0.48
17918	663.552	18.40	0.69
17918	689.434	17.11	0.90
17918	692.396	18.08	0.90
21770	663.500	−46.18	0.28
21770	689.444	−46.35	0.48
21770	692.469	−46.01	0.28
24832	663.538	20.61	1.56
24832	692.433	18.20	0.90
24832	693.569	22.67	0.69
30020	663.570	34.31	0.69
30020	692.567	37.19	0.48
30020	693.609	37.87	0.90
34045	663.591	29.89	0.48
34045	689.467	26.19	0.94
34045	692.587	29.18	0.48
48737	663.606	26.12	0.90
48737	665.620	26.30	0.48
48737	689.459	25.77	0.48
48737	692.598	27.35	0.69
48737	693.630	27.56	0.48
50019	663.611	31.17	0.69
50019	664.643	30.75	0.69
50019	665.626	30.30	0.69
50019	692.601	30.04	0.69
50019	693.633	32.39	0.90
60489	663.617	52.67	0.69
60489	665.645	53.42	0.69
60489	692.608	30.81	0.48
60489	693.650	31.65	0.28
62437	663.627	11.13	0.48
62437	665.677	14.46	1.34

Table 3. continued

HD	HJD (+2449000)	V_r km s^{-1}	I km s^{-1}
62437	692.628	15.99	0.28
62437	693.639	14.12	0.69
69997	663.642	31.67	0.28
69997	692.641	32.79	0.28
69997	692.703	33.18	0.28
69997	693.661	32.59	0.28
82043	663.652	12.25	0.48
82043	692.649	1.73	0.69
82043	692.712	1.41	0.69
82043	693.679	0.14	0.48
84607	663.660	13.65	0.48
84607	692.660	12.25	0.69
84607	692.723	13.50	0.69
84607	693.690	13.09	0.48
86611	663.688	26.47	0.90
86611	692.669	24.42	0.90
86611	692.732	25.79	0.69
86611	693.699	25.04	1.34
89025	692.676	−21.20	0.69
89025	693.710	−22.07	0.28
92787	692.689	4.47	0.90
92787	692.692	4.47	0.90
92787	693.715	3.82	0.48
100418	470.406	1.02	0.69
100418	471.327	0.76	0.58
100418	471.390	−0.57	0.69
100418	472.398	2.28	0.28
100418	473.336	0.22	0.69
100418	474.359	−1.81	0.48
100418	506.372	−0.28	0.28
103313	470.461	16.10	0.69
103313	471.340	16.75	0.48
103313	471.463	14.71	0.28
103313	472.413	19.14	0.90
103313	473.359	17.59	0.69
103313	473.440	17.88	0.90
103313	474.378	16.54	0.69
103313	474.414	16.72	0.48
103313	505.387	22.17	1.56
103313	507.364	18.64	0.48
103313	507.397	15.74	2.01
104827	470.475	10.21	0.48
104827	471.352	8.07	0.90
104827	471.399	7.33	0.48
104827	472.443	7.70	0.48
104827	473.373	7.60	0.48
104827	473.482	8.42	0.48
104827	474.332	7.37	0.69
104827	474.479	6.93	0.48
104827	506.394	8.89	0.48
108382	470.486	−2.33	0.48
108382	471.364	−1.97	0.48
108382	471.471	−1.82	0.48
108382	472.457	−2.86	0.69
108382	473.383	−1.97	0.90
108382	473.430	−2.71	0.69
108382	474.345	−1.55	0.90

Table 3. continued

HD	HJD (+2449000)	V_r km s^{-1}	I km s^{-1}
118295	470.535	−20.00	0.69
118295	471.375	−19.63	0.69
118295	471.447	−17.52	1.56
118295	472.470	−20.59	0.69
118295	473.401	−18.46	0.94
118295	474.394	−17.76	0.69
118295	505.410	−24.23	0.94
118295	506.420	−19.84	1.34
108382	474.446	−1.89	0.90
122703	470.522	−17.63	0.69
122703	471.430	−13.34	0.90
122703	471.485	−21.60	0.69
122703	472.509	−19.21	2.01
122703	473.455	−15.39	0.69
122703	474.464	−17.16	0.94
150453	471.521	0.82	0.69
150453	471.620	0.47	0.69
150453	472.586	0.12	0.28
150453	473.541	0.64	0.48
150453	474.568	−0.10	0.28
150453	506.486	1.54	0.28
150557	471.510	−49.75	0.48
150557	472.492	−49.42	0.69
150557	473.496	−48.36	0.90
150557	474.494	−49.64	0.69
150557	474.540	−50.22	0.48
150557	505.532	−48.20	0.48
150557	506.412	−48.49	0.94
150557	506.467	−50.15	0.28
150557	509.393	−49.60	0.48
155646	470.552	59.76	0.48
155646	471.535	61.08	0.48
155646	472.542	62.36	0.48
155646	473.518	59.78	0.28
155646	474.524	58.64	0.48
155646	505.545	60.05	0.48
155646	506.445	59.95	0.28
155646	506.547	60.70	0.28
159561	470.565	10.69	0.69
159561	471.543	11.10	0.48
159561	472.550	12.23	0.69
159561	472.631	10.25	0.94
159561	473.527	12.03	0.90
159561	474.510	10.82	0.69
159561	505.431	11.46	0.90
159561	506.457	10.65	0.48
159561	507.608	9.68	0.69
159561	509.446	8.29	0.48
171856	470.639	−5.56	2.01
171856	473.620	−5.96	1.34
171856	506.584	−21.70	0.48
171856	508.544	−19.14	0.69
174866	470.625	−39.39	0.94
174866	472.615	−38.50	0.69
174866	473.606	−40.45	0.48
174866	505.585	−40.89	0.90
174866	506.571	−43.56	1.34
174866	509.521	−42.08	0.69

Table 3. continued

HD	HJD (+2449000)	V_r km s^{-1}	I km s^{-1}
176971	470.575	−34.62	0.90
176971	471.553	−34.28	0.48
176971	472.559	−31.63	0.69
176971	473.560	−35.13	0.48
176971	474.579	−33.63	0.69
176971	474.625	−34.88	1.34
176971	505.461	−34.60	0.94
176971	506.517	−32.51	0.69
176971	509.414	−29.47	1.78
177392	470.608	10.13	0.48
177392	471.577	9.51	1.56
177392	472.603	12.38	0.69
177392	473.580	10.12	0.90
177392	474.593	6.75	0.90
177392	505.481	11.21	0.90
177392	506.502	10.31	2.01
177392	508.525	6.75	0.90
177392	509.459	8.69	0.28
177392	509.539	7.37	0.90
178187	470.600	−24.85	0.69
178187	471.563	−24.43	0.69
178187	472.568	−24.82	0.48
178187	473.570	−25.11	0.94
178187	474.602	−24.69	0.90
178187	505.440	−24.69	0.69
178187	505.518	−25.04	0.90
178187	506.531	−25.03	0.90
178187	507.585	−22.70	0.48
178187	508.506	−23.06	0.69
186005	472.623	−40.39	1.34
186005	474.634	−39.98	0.90
186005	506.593	−39.50	0.90
186005	509.593	−42.63	0.48
187764	471.598	−8.02	0.69
187764	473.589	−5.96	0.48
187764	474.551	−8.39	0.90
187764	474.612	−4.71	0.90
187764	505.560	−6.14	0.69
187764	506.554	−3.10	0.69
187764	509.477	−4.64	0.69
190172	471.628	2.82	0.48
190172	473.628	6.00	0.28
190172	506.602	3.11	0.48
203842	663.228	−25.94	0.69
203842	665.246	−27.74	0.48
203842	690.313	−26.43	0.69
203842	692.296	−24.73	0.90
203842	693.243	−23.22	0.48
204577	663.245	−10.45	0.48
204577	693.273	−8.69	0.69
205852	663.262	−31.90	0.90
205852	692.307	−31.83	0.69
205852	693.308	−32.48	0.69
209166	663.275	5.22	0.28
209166	692.314	6.36	0.28
209166	693.322	6.82	0.48

Table 3. continued

HD	HJD (+2449000)	V_r km s^{-1}	I km s^{-1}
210516	663.295	10.46	0.69
210516	692.332	11.38	0.94
210516	693.339	12.16	0.94
216701	663.314	12.70	0.48
216701	692.352	15.26	0.69
216701	693.355	11.36	0.48
217131	663.334	−12.12	0.28
217131	693.374	−11.35	0.48
219891	663.352	−3.04	0.90
219891	689.338	−3.01	2.01
219891	693.396	−0.48	0.94
224995	663.383	8.13	0.48
224995	689.302	7.14	0.90
224995	693.431	7.48	0.69

compute the residuals to the regression line fitting the cumulative distribution. The α parameter corresponding to the minimum residuals is then adopted. Figure 5 shows the behaviour of the rms deviation of the residuals as a function of α. A minimum clearly appears around $\alpha = 1.2$. This means that the error on $\sigma^{\rm s}_{V_r}$ is underestimated by about 20%, which is quite reasonable considering the numerous uncertainties affecting its determination. Figure 6 shows the histogram and cumulative distribution of $P(\chi^2)$ for $\alpha = 1.2$, as well as the straight line minimising the residuals of the cumulative distribution.

According to this criterion, 52% of the stars are variable and are listed in Table 4; the others are listed in Table 5. Each table gives the spectral type, $P(\chi^2)$, the blanketing parameter Δm_2, $v \sin i$ and eventually some remarks. The source of the projected rotational velocities is Abt & Morrell (1995) or the Bright Star Catalogue (BSC), except for HD 6706, HD 122703, HD 150453, HD 190172 and HD 217131 whose $v \sin i$ is determined by the optimum fit of a synthetic spectrum to our observed spectra. The spectral types are taken from Hauck (1986) who refers to Cowley et al. (1969), Cowley (1976), the Michigan catalogue (Houk & Cowley 1975; Houk 1978, 1982), Jaschek (1978) and the BSC. Δm_2 are taken from the Geneva photometry database. The values can differ from those of Hauck (1986) because new measurements have been made and a new reference sequence for the Hyades has been defined (see Sect. 5.1). The Δm_2 value can be weaker by a few thousandths of magnitude in the most unfavourable cases for visual doubles. This effect can only diminish the sample of metallic F giants, while the sample of metallic giants cannot be polluted by non-metallic stars. Remarks D and SB come from the BSC.

The stars HD 2628 (3 measurements), HD 10845 (2), HD 11522 (2), HD 24832 (3), HD 62437 (4), HD 69997 (4), HD 1772392 (10) and HD 187764 (7) belong to the

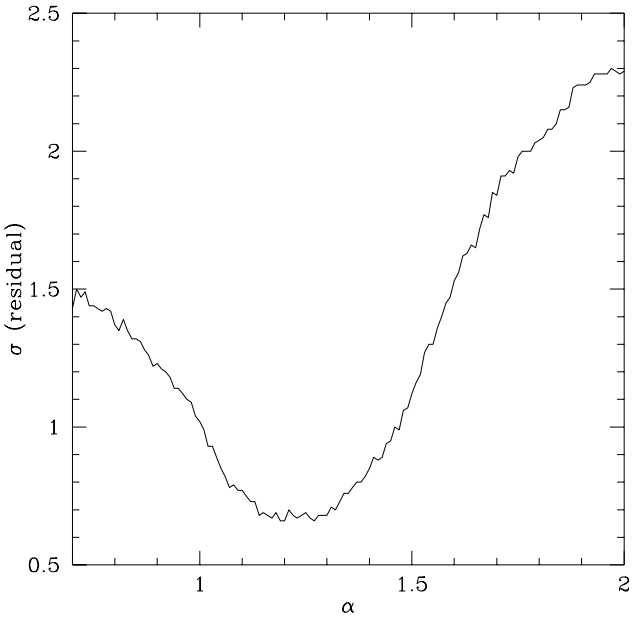

Fig. 5. Standard deviation of the residuals as a function of the α parameter

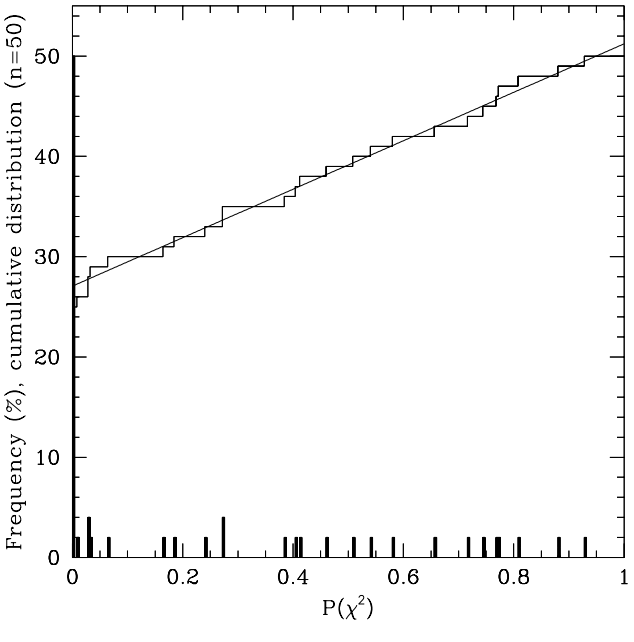

Fig. 6. Histogram and cumulative distribution of the $P(\chi^2)$ for the 50 A and F giant stars. These distributions correspond to an α parameter of 1.2 ensuring a flat distribution between 0 and 1. We have also drawn the straight line determined by a least-squares fit of the cumulative distribution

catalogue of δ Scuti stars of Rodriguez et al. (1994). In principle, all of these stars should be detected as variable, but the first three are not. For these, we have only a few measurements separated by several days. As ill luck would have it, for HD 2628 and HD 11522 the exposures are made at the same pulsational phase. For HD 10845, our measurements cover different phases, but the small amplitude of the lightcurve (0.02 mag in the V filter) is probably responsible for the non-detection. For the five δ Scuti stars detected, we find an average ratio of 110 $\mathrm{km\,s^{-1}\,mag^{-1}}$ between the peak-to-peak radial velocity and photometric variations, which is compatible with the value of 92 $\mathrm{km\,s^{-1}\,mag^{-1}}$ given by Breger (1979). Therefore, it seems that the V_r variation of these five objects is only due to pulsation and not to any orbital motion.

Among the stars not detected as variable, five are listed as SB in the BSC: HD 50019, HD 84607, HD 86611, HD 89025 and HD 92787. Low spectroscopic dispersion ($30-40$ $\mathrm{\AA\,mm^{-1}}$) and fast rotational velocity may probably explain the large variations reported in the past. Figure 7 shows for these five stars the rms scatter of the radial velocities in the literature as a function of $v \sin i$. For HD 89025, we did not take into account the measurements made by Henroteau (1923), because they differ systematically from the others and would generate an artificially larger dispersion. For the older measurements, there is a clear correlation between dispersion and rotation: when $v \sin i$ increases from 70 to 215 $\mathrm{km\,s^{-1}}$, σ increases from 7 to 25 $\mathrm{km\,s^{-1}}$. Our mean radial velocities values are compatible with the older ones, except for HD 86611 which rotates very fast.

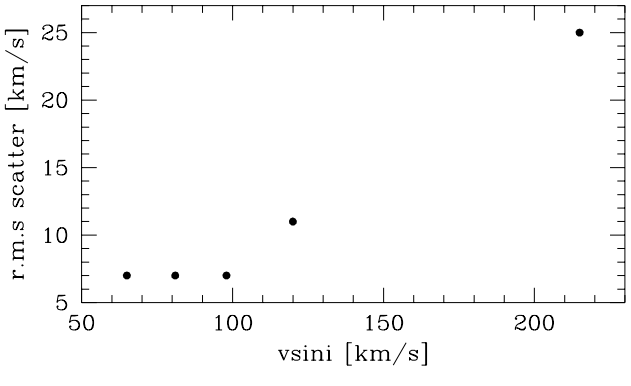

Fig. 7. Rms scatter of the V_r as a function of $v \sin i$ for stars considered as SB in the BSC but not detected variable in this paper

In Fig. 8, we show the behaviour of the external scatter E (which is equivalent to the dispersion of the measurements) as a function of $v \sin i$ for the fifty giant stars and the seven standards of the programme. Black and open symbols represent respectively non variable and variable stars on the basis of the $P(\chi^2)$. A linear regression including only non-variable stars is also represented. This straight line is, as a first approximation, the mean internal error I as a function of $v \sin i$ and agrees well with the values determined previously. Most of the variable stars clearly appear above this line and then we could also use it as criterion of variability.

Table 4. Detected variable stars

HD	Spectral type	$P(\chi^2)$	Δm_2	$v \sin i$	Remarks
4338	F2III	0.000	0.009	98	D
24832	F1V	0.000	0.004	150	δ Scuti
30020	F4IIIp	0.000	0.089	60	SB
34045	F2III	0.001	0.021	67	
60489	A7III	0.000	0.008	15	
62437	F0III	0.000	0.008	35	δ Scuti
69997	F2III	0.000	0.042	25	δ Scuti
82043	F0III	0.000	0.003	51	
100418	F9III	0.000	−0.020	33	
103313	F0V	0.000	0.009	61	
104827	F0IV-V	0.000	0.002	38	SB,D
118295	A7-F0V	0.000	−0.003	135	
122703	F5III	0.000	0.008	69	
150453	F4III-IV	0.001	−0.033	10	
155646	F6III	0.000	−0.034	$\leq$10	
159561	A5III	0.000	−0.019	210	SB
171856	A8IIIn	0.000	−0.001	110	D
174866	A7Vn	0.001	−0.012	150	
176971	A4V	0.000	−0.016	125	
177392	F2III	0.000	0.030	120	δ Scuti
186005	F1III	0.003	0.006	140	SB
187764	F0III	0.000	−0.003	85	δ Scuti
190172	F4III	0.000	−0.001	25	
203842	F5III	0.000	−0.006	84	
209166	F4III	0.001	0.007	<20	D
216701	A7III	0.000	−0.005	80	

δ-Scuti type stars are represented by triangles, the most variable of them having an external scatter of about 1.8 km $\mathrm{s^{-1}}$, which is reasonable for stars with an amplitude of 0.05 mag. We can see that most of the variable stars have an external scatter below 1.8 km $\mathrm{s^{-1}}$ and so the origin of this variability remains ambiguous. Some of them are intrinsic variables not as yet classified δ Scuti. Only stars with $E \geq 2$ km $\mathrm{s^{-1}}$ can be considered as binaries with a high probability.

4.2. Rate of detection

We have made a simulation to determine the rate of detected variable stars as a function of the period. For this, a sample of 1000 double stars with given periods was created as a first step. A flat distribution of the mass ratio was assumed (Mazeh et al. 1992) with primary components of A and F types ($1.5-3$ $M_\odot$). The orbital elements T_0, ω and i are randomly distributed, while the eccentricity is distributed according to Duquennoy & Mayor (1991): when the period is less than 10 days, the orbit is assumed to be circular; for periods between 10 and 1000 days, the eccentricity is distributed following a gaussian with a mean equal to 0.3 and $\sigma = 0.15$ (cases with negative eccentricity were dropped and replaced); for longer periods, the

Table 5. Non-variable stars

HD	Spectral type	$P(\chi^2)$	Δm_2	$v \sin i$	Remarks
1671	F5III	0.929	0.002	41	
2628	A7III	0.510	−0.004	18	δ Scuti
6706	F5III	0.746	−0.003	50	
10845	A9III	0.770	0.015	85	δ Scuti
11522	F0III	0.581	−0.009	120	δ Scuti
12573	A5III	0.275	−0.017	95	
17584	F2III	0.656	0.015	149	
17918	F5III	0.461	0.033	120	
21770	F4III	0.808	−0.023	29	
48737	F5III	0.065	0.008	70	
50019	A3III	0.275	−0.006	120	SB
84607	F4III	0.388	0.023	98	SB
86611	F0V	0.415	−0.015	215	SB
89025	F0III	0.242	0.038	81	SB
92787	F5III	0.719	−0.023	65	SB
108382	A4V	0.881	0.006	65	
150557	F2III-IV	0.031	−0.009	67	
178187	A4III	0.032	−0.003	35	
204577	F3III	0.036	0.008	$\leq$15	
205852	F3III	0.775	0.020	155	
210516	A3III	0.407	−0.017	40	
217131	F3III	0.166	−0.016	66	
219891	A5Vn	0.186	−0.007	175	
224995	A6V	0.543	−0.009	90	

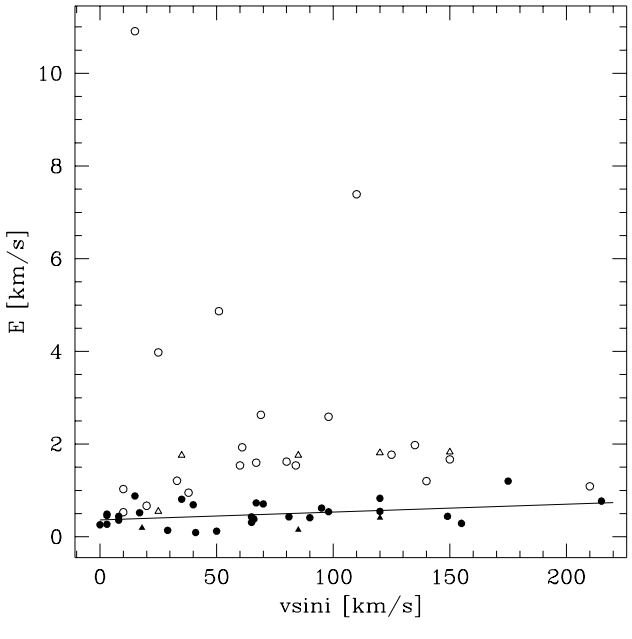

Fig. 8. External scatter E as a function of $v \sin i$. Stars with $P(\chi^2) > 0.01$ are represeted by black symbols and with $P(\chi^2) \leq 0.01$ by open symbols. δ Scuti type stars are represented by triangles. A linear regression is shown for constant stars

distribution $f(e) = 2e$ is assumed. In a second step, the radial velocities of the created sample are computed at the epochs of observation of the real programme stars. Then a random internal error is added to these 50000 radial velocities. Finally the $P(\chi^2)$ value of each star is computed and we can take the census of detected binary stars for a given period. The results are presented in Fig. 9 for periods between 1 and 10^5 days.

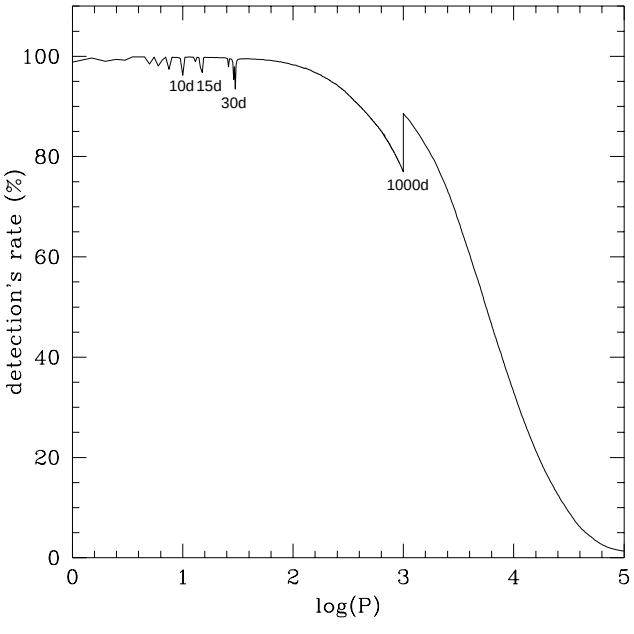

Fig. 9. Detection rate as a function of the period. P is given in days

The simulated detection rate is very high for systems with periods below 100 days: it varies between 93.5% and 99.9%. Above 100 days, the rate decreases rapidly, being about 80% for 1000 days and 30% for 10000 days. The discontinuity which appears for 1000 days is due to the strong change in the distribution of eccentricities: indeed, from this point on we grant more importance to large e. The size of this effect is related to the time distribution of the measurements. For instance, if the exposures were more distant in time, the discontinuity would be smaller. The simulation shows some very peaked depressions at shorter periods: at $P = 30$ days, which corresponds to the time interval between two successive observing runs and at dividers of 30, i.e. 15, 10, 7.5, 6 and 5 days. This is completely normal, because for such periods, the time distribution of the measurements makes the detection of binary stars less efficient. At $P = 3$ days and $P = 2$ days, the rate remains very high, because each run lasts for about 4 or 5 days. At $P = 10$ days, there is a weak discontinuity due to the change of distribution of eccentricity, but this effect is hidden inside the peak.

In addition, we have computed the mean rate of detection among binaries with periods less than 100 days. The binaries are created as before but the periods are distributed as a gaussian with a mean equal to $\overline{\log(P)} = 4.8$ and $\sigma_{\log(P)} = 2.3$ (Duquennoy & Mayor 1991), where P is given in days. When cut-offs at 1 and 100 days were imposed, the detection rate reached 99%, i.e. all close binaries are detected. The rate remains as high as 94% for periods between 1 and 1000 days.

5. Comparison between Am stars and F giants

Before discussing the rotation and the rate of binaries among Am and giant A-F stars, it is useful to consider again the mean value of the blanketing parameter Δm_2 for Am stars as well as the range of spectral types of giant metallic stars.

5.1. Parameter of metallicity Δm_2

In the $B2 - V1$ vs. m_2 diagram, the Am stars are located above the reference sequence defined by the Hyades (Hauck 1973). The difference Δm_2 is interpreted in terms of metallicity. Hauck & Curchod (1980) have determined the mean value of Δm_2 for classical Am stars ($g \geq 5$, where g is the difference between the spectral type deduced from the metallic lines and that from the K line) and for mild Am stars ($g < 5$) and have obtained respectively 0.013 ± 0.019 (146 stars) and 0.002 ± 0.011 (23 stars). They considered only objects brighter than the 7th magnitude in order to avoid any significant interstellar reddening.

Since then, a new sequence of reference has been defined (Hauck et al. 1991) taking into account new observations of the Hyades. This new sequence is different from the old one mainly for stars with a type later than F; for early A type stars the old and new sequences are identical, while for late A and F stars they are separated by only a few thousandths of a magnitude. Taking into account the stars of the revised catalogue of Curchod & Hauck (1979) brighter than the 7th magnitude, the new values are $\overline{\Delta m_2} = 0.011 \pm 0.021$ (238 stars) and $\overline{\Delta m_2} = -0.001 \pm 0.025$ (101 stars) for classical and mild Am respectively, i.e a decrease of about 2 or 3 mmag with respect to the preceding values. Therefore, a giant star will be considered here as metallic whenever its Δm_2 is larger than or equal to 0.013, rather than 0.015 as defined by Hauck & Curchod (1980).

5.2. Spectral types of metallic giants

The diagram Δm_2 vs. $T_{\rm eff}$ for giant A-F stars of Hauck (1986) is shown again in Fig. 10. The effective temperature is deduced from the semi-empirical calibrations of Künzli et al. (1997). Notice that only F stars have an enhanced Δm_2 value while this property never applies for A-type stars. Indeed, all stars with $\Delta m_2 \geq 0.013$ have types between F0 and F6, except for HD 10845, HD 90277 and HD 147547 which are classified A9 and HD 4849 which is classified A9/F0. The lack of metallic stars later than F6 is explained by the diffusion theory: Vauclair & Vauclair (1982) have defined the limit where the diffusion time scale for helium at the bottom of the surface convective zone equals the stellar lifetime in a $\log(L/L_\odot)$ vs $\log(T_{\rm eff})$ diagram; this limit crosses the area of giants at $\log(T_{\rm eff}) = 3.8$, which fits exactly the limit we find in our diagram. It is most interesting to notice that several metallic giants also are δ Scuti stars, because Am peculiarity and δ Scuti-type pulsation are mutually exclusive. Only mild Am stars may be δ Scuti, as well as δ Del stars. In this respect, the metallic F giants are completely similar to δ Del stars (Kurtz 1976).

The study of a relation between Am stars and metallic A-F giants is now restricted between Am and metallic giant F0-6 stars. In the next two section, we compare rotation and duplicity among these two samples.

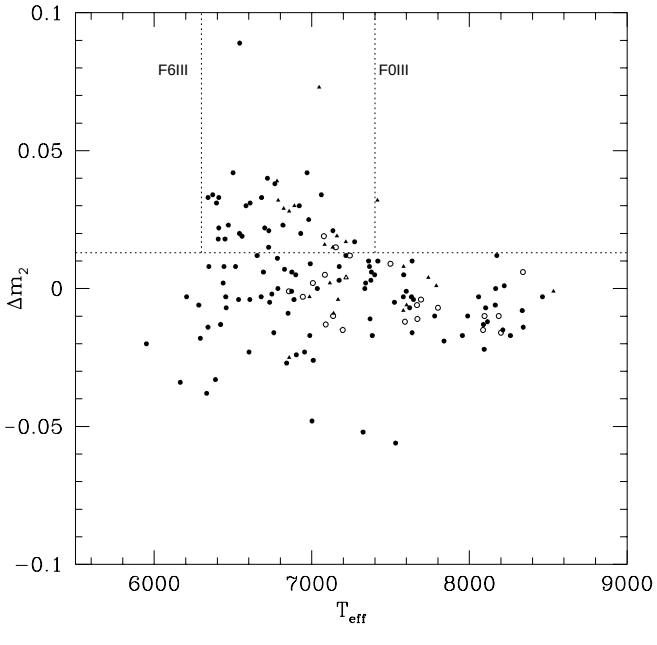

Fig. 10. Δm_2 vs. $T_{\rm eff}$ diagram for A-F giants of Hauck (1986). The black dots represent spectroscopic giant stars and open dots photometric giants ($\Delta d \geq 0.12$). δ Scuti stars are represented by triangles, the others by circles. The horizontal line separates metallic stars from normal ones. The two vertical lines at 6300 K and 7400 K define the red and blue limits for metallic giants

5.3. $V \sin i$ of Am and metallic F0-6III

The Am stars are taken from the revised catalogue of Curchod & Hauck (1979). Their $v \sin i$ used is an

average of the values given by Abt & Levy (1985), Uesugi & Fukuda (1978, 1982), Bernacca & Perinotto (1971), Boyarchuk & Kopylov (1964). For stars with four measurements, we obtain a standard deviation of about 9 km s^{-1} which is a first indication of the precision of these $v \sin i$. The projected rotational velocities of metallic F0-6III stars are taken from Abt & Morrell (1995) or the BSC (28 stars). Abt & Morrell (1995) give an error on the determination of the radial velocity of about 10 km s^{-1}. To make the comparison meaningful, we take into account only the Am stars brighter than the 7th magnitude and with $\Delta m_2 \geq 0.013$ (98 stars). The Am stars with a low Δm_2 value have underabundant scandium and calcium, and normal or slightly overabundant heavier elements. On the other hand, F0-6III stars with low Δm_2 have a normal chemical composition, so there is no similarity between these two categories.

We present in Fig. 11 the histograms and cumulative distributions of the projected rotational velocities for the Am and metallic F0-6III stars, and the cumulative distribution for non metallic FIII stars. Obviously, Am stars (full line) and metallic F0-6 giants (dotted line) do not follow the same distribution. The $v \sin i$ of Am stars are below 100 km s^{-1} except for one star, while those of F giants are often faster than 100 km s^{-1}. The maximum of the distribution for Am star is between 30 and 40 km s^{-1}; for F giants, the distribution seems flat with a cut-off at about 160 km s^{-1}.

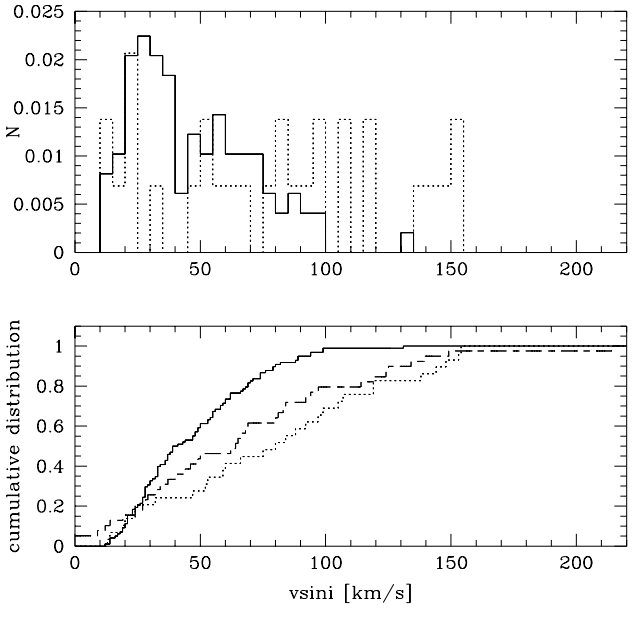

Fig. 11. Comparison between the distributions of $v \sin i$ for Am stars (full line) and metallic F0-6III stars (dotted line). We have also given the cumulative distribution for giant non-metallic F stars (broken line). Histograms and cumulative distributions are normalised

Cumulative distributions give more satisfactory information than histograms because they do not depend on the width of the bins. We have applied the Kolmogorov-Smirnov test to the distributions of the Am stars and of the metallic giants: adopting the H_0 hypothesis that they are identical, one obtains the probability $P = 3.692\ 10^{-4}$ to have a test value at least as extreme as the actually observed one. Therefore we can reject the H_0 hypothesis at the 99% confidence level and the distributions are very probably not similar. In the sample of F giants, some δ Scuti stars are present; in the framework of the scenario where Am stars are progenitors of metallic F giants, this implies that Am stars may pulsate as soon as they have evolved into giants. This assumption is based on the fact that some δ Del stars do pulsate and may be evolved Am stars (Kurtz 1976). If this assumption is wrong, then the sample of metallic giants is polluted. For that reason, we have applied the test used above to Am and F giants not known as δ Scuti stars and found $P = 6.227\ 10^{-4}$, which does not change the conclusion.

The Kolmogorov-Smirnov test applied to metallic and non-metallic FIII stars gives a P value of 0.46. So there is no real difference between these two samples from the point of view of projected rotational velocities, contrary to what we observe between Am and normal A dwarf.

5.4. Rate of binaries among Am and metallic F0-6III

Let us discuss now the rate of close binaries with periods below 1000 days among metallic F0-6 giants.

Since there are only 10 such stars in our sample of stars measured with Aurélie, we have to rely largely on results published in the literature. Table 6 lists some remarks about these data for each of the 41 metallic giants. For HD 4919 and HD 177482, however, the V_r data are too poor and inaccurate. Only 39 stars have therefore been retained, of which 6 stars are strictly speaking members of tight binaries: HD 30020, HD 34045, HD 43905, HD 85040, HD 108722 and HD 110318, which constitute 15.4% of the sample. For some other stars, the decision is less clear-cut. For fast rotators, it is difficult to know whether the observed dispersion is just due to the large $v \sin i$ or betrays an orbital motion; this is especially the case of HD 13174 and HD 147547. For the δ Scuti stars HD 214441, we observe a ratio of about 200 km s^{-1}mag^{-1} between the peak-to-peak radial velocity and photometric variation which is double the value given by Breger (1979). Thus the additional variation in radial velocities could be due to orbital motion. But if these three stars are added to the sample of tight binaries, the proportion would only increase to 23.1% and to 23.3% if we take only F giants not known as δ Scuti type stars. These values are the observed rates; the real rates must be only slightly higher because the fraction of undetected stars is weak for small periods. It is interesting to note that the observed rate

agrees with the value for solar-type stars in the vicinity of the Sun, i.e. 21.7% (Duquennoy & Mayor 1991) for $P \leq$ 1000 days.

Table 6. Discussion about the duplicity of all photometric metallic F giant stars of Hauck (1986).

HD 1324:
Single star (Evans et al. 1964).

HD 2724:
δ Scuti (Rodriguez et al. 1994). The V_r measurements of Nordström & Andersen (1985) show no variation.

HD 4849:
δ Scuti (Rodriguez et al. 1994). The V_r measurements of Nordström & Andersen (1985) show no variation.

HD 4919:
δ Scuti (Rodriguez et al. 1994). As we only have an old V_r from the catalogue of Campbell (1913), we cannot conclude about the duplicity.

HD 10845:
δ Scuti (Rodriguez et al. 1994). Our measurements show no variation.

HD 12311:
From his 15 exposures, Campbell (1928) indicated that this star is probably variable. At the time, he had only a few broad lines. Catchpole et al. (1982) observed no variation from 4 measurements. They obtained a mean radial velocity of 15.2 ± 3.1 km s^{-1}.

HD 13174:
Campbell (1928) obtained values covering a large interval $[-10, +20$ km s$^{-1}]$. This dispersion is probably due essentially to a fast rotation ($v \sin i$ =154), nevertheless we cannot exclude a close companion. Adams et al. (1929) and Abt (1969) gave coherent velocities of about -6 km s^{-1}.

HD 15233:
The comparison between values obtained by Campbell (1913, 1928) and by Buscombe & Morris (1958) shows that this star must be a binary with a long period. Indeed, these authors gave very different radial velocities: one found positive velocities, the others negative velocities, with a very good internal coherence if we consider the high rotation ($v \sin i = 106$ km s^{-1}). We find a value of $P(\chi^2)$ of 0.08 for the measurements of Buscombe & Morris (1958) showing, according to this criterion, that no variation is detected on a scale of 700 days.

HD 17584:
Our measurements show no variation. We obtain a velocity of 18 km s^{-1} and Campbell (1913) 14 km s^{-1}.

HD 17918:
Our measurements show no variation as is the case of the measurements of Shajn & Albitzky (1932).

HD 30020:
The measurements made at OHP are compatible with the preceding ones of Adams et al. (1929) and Abt (1969). The available values are distributed between 34.40 km s^{-1} and 41.50 km s^{-1} with a characteristic time variation of about 0.7 km s^{-1}/day taking into account our measurements of December 1994. The variability is certainly due to an orbit because the photometric variations are less than 1 mmag in the filter B and V of Johnson (Nelson & Kreidl 1993).

HD 33276:
The measurements of Campbell (1928) and Abt (1965) show no variation.

HD 34045:
If we put together our measurements and those of Nordström & Andersen (1985), the velocity varies between 26.32 and 34.70 km s^{-1}. The characteristic time of variation is 0.95 km s^{-1}/day for our measurements (3 days between two measurments) and 0.91 km s^{-1}/day for Nordström & Andersen (1985) (5 days between two measurements). As this star is not known as a δ Scuti, we think it is a tight binary.

HD 40455:
For this star, we have only 3 measurements of Nordström & Andersen (1985) on a scale of 300 days. The $P(\chi^2)$ is 0.74 and so this star is probably not a tight binary.

HD 43905:
SB1 with a period of 6.5 days (Mayor & Mazeh 1987).

HD 59881:
The $P(\chi^2)$ is 0.06 and 0.13 for the measurements of Frost et al. (1929) et Penfold (1983) respectively. So this star is probably not a binary with a small period.

HD 61064:
If we put together the measurements of Campbell (1913, 1928) and those of Shajn & Albitzky (1932), the mean value of the radial velocity is 45.72 km s^{-1} with a dispersion of 1.72 km s^{-1}, so we observe no tangible variation.

HD 61110:
The measurements taken from Campbell (1913, 1928), Harper (1937), Buscombe & Morris (1958), Abt (1969) give a mean radial velocity of 6.5 km s^{-1} and a dispersion of 3.5 km s^{-1} for 13 data. The dispersion is not so large if we consider the quite large rotational velocity (90 km s^{-1}). So this star is probably not a tight binary.

HD 69997:
δ Scuti (Rodriguez et al. 1994). Our measurements allow to detect intrinsic variations but no orbital motion.

HD 79940:
Single star (Evans et al. 1961). This star is noted SB in the BSC. This probably comes from Abt & Biggs (1972). Indeed, in addition to the authors mentioned above who find a radial velocity of 2.2 ± 1.5 km s^{-1}, they list Campbell (1928, p. 143), who found a radial velocity of 12 km s^{-1} based on 3 measurements. The large rotational velocity probably explains the discrepancy.

HD 84607:
We detect no variation of this star at OHP. We obtain a mean radial velocity of 13 km s^{-1} which is compatible with the value of 16.3 ± 2 given by Shajn & Albitzky (1932). Wilson & Joy (1950) and Abt (1969) both found important fluctuations of velocity, which are spurious, probably due to the rotation. In both cases, the mean value is 13.4 km s^{-1}. The SB notation in the BSC seems to be a premature decision.

HD 85040:
δ Scuti (Rodriguez et al. 1994). SB2 with a period of 4.14 days (Rosvick & Scarfe 1991)

HD 89025:
The data since the beginning of the century show a radial velocity variation about 50 km s^{-1}, but no short-term variation is detected, so it is probably not a tight binary as is suggested in the BSC. Indeed, apart from the values of Henroteau (1923) who obtained a mean velocity of about -54 km s^{-1}, the others have radial velocities between -30 and 0 km s^{-1} with a mean of -17 km s^{-1}. This scatter is probably due both to the quite large $v \sin i$ (81 km s^{-1}) and the low dispersion of the spectra (≈ 30 Å/mm). The computation of the $P(\chi^2)$ gives 0.88 and 0.53 for the measurements of Jones & Haslam (1969) and Wooley et al. (1971) respectively, and 0 for the old measurements of Abt (1969). Our radial velocities are compatible with those of Adams et al. (1929) who obtained -19.3 ± 2.9.

HD 89254:
The measurements given by Adams et al. (1929), Buscombes & Morris (1958), Abt (1969) and Evans et al. (1961) suggest a constant radial velocity ($\overline{V_r} = 15.8 \pm 4.4$). This dispersion is compatible with a rotational velocity of 76 km s^{-1}.

HD 90277:
This star shows no variation. The mean velocity is 13.6 km s^{-1} with a dispersion of 2.7 km s^{-1} from the 36 measurements taken from 9 different authors.

HD 90454:
From the measurements of Cannon (1920) and those of Nordström & Andersen (1985), the $P(\chi^2)$ is 0.31 and 0.03 respectively and so it is probably not a binary.

HD 105841:
Single star (Evans 1966).

HD 108722:
SB1 with a period of 17.954 days (Abt & Levy 1976).

HD 110318:
SB2 with a period of 44.4 days (Sanford & Karr 1942).

HD 115604:
δ Scuti (Rodriguez et al. 1994). On a time span of about 130 days, Smith (1982) observes a variation of radial velocity of 6.2 km s^{-1}. Such a variation is probably due to pulsation only.

HD 125150:
Single star (Evans et al. 1964).

HD 126251:
Single star (Wilson & Joy 1950).

HD 147547:
Radial velocities are distributed between -60 and -30 km s^{-1} with a mean of about -44 km s^{-1}. The large dispersion is probably due to the fast rotation of 145 km s^{-1}, nevertheless we cannot exclude a contribution of a companion.

HD 157919:
It shows no variation. The mean radial velocity is 37.2 ± 2.4 km s^{-1} for 14 measurements taken from Campbell (1913), Campbell (1928), Shajn & Albitzky (1932), Evans et al. (1957)

HD 177392:
δ Scuti (Rodriguez et al. 1994). Our measurements allow to detect intrinsic variations but no orbital motion.

HD 177482:
δ Scuti (Rodriguez et al. 1994). Campbell (1928) obtains values covering a large interval [+3, +26 km s^{-1}] with the remark "poor lines" and Neubauer (1930) gives a value of 6.5 km s^{-1}. With these old values, it is difficult to say anything about the duplicity.

HD 181333:
δ Scuti (Rodriguez et al. 1994). On a time span of about 38 days, Smith (1982) observes a variation of radial velocity of 4.7 km s^{-1}. Such a variation is probably due to pulsation only.

HD 196524:
Binary star with a probable period of 26.65 years (Abt & Levy 1976). So it will not be integrated in the sample of close binaries.

HD 205852:
From the $P(\chi^2)$ value, the measurements of Frost et al. (1929), Jones & Haslam (1969) and this paper show no variations.

HD 208741:
Single star (Buscombe & Morris 1958 and Evans et al. 1964).

HD 214441:
δ Scuti with a variation of 0.05 mag in visual magnitude (Rodriguez et al. 1994). Nordström & Andersen (1985) find a ΔV_r of about 10 km s^{-1} and we then obtain a ratio of 200 km s^{-1}mag^{-1} which is large in comparison with the value of 92 km s^{-1}mag^{-1} given by Breger (1979). We cannot therefore exclude a companion for this star.

In their paper of 1985, Abt & Levy estimated that the number of Am stars in double systems with periods less than 1000 days represents 75% of the sample, i.e. a rate considerably larger than what we find for metallic F giants. This is an additional reason to reject the possibility of any evolutionary link between Am stars and metallic F giants.

The upper limit of the fraction of binary stars among the forty non-metallic A and F giant stars measured at OHP is 47%. This value is enhanced because it certainly includes some unrecognised intrinsic variables. Of the 113 stars of this category (Hauck 1986), 24 are classified as SB, 11 have a variable radial velocity (V) and 6 are suspected variables (V?) in the BSC. The fraction of binaries with a small period among this type of stars is between 21.2% (SB only) and 36.3% (SB + V + V?) which may include some intrinsic variables. Thus frequencies of binaries with small periods among metallic and non-metallic A and F giant stars are not so different from each other, contrary to the case of Am and normal A dwarfs.

6. Conclusion

From the point of view of observed chemical abundances and of the theory of radiative diffusion, the scenario which considers Am stars as progenitors of metallic F0-6 giants is completely justified. It was worth the effort to try to settle this idea on firmer grounds, or alternatively to question it, by considering two other fundamental characteristics of Am stars, namely slow rotation and high rate of binaries. The main results of our work may be summarised as follows:

- Giant A-type stars never show an enhanced photometric metallicity, i.e $\Delta m_2 \geq 0.013$. Therefore, if they are descendants of Am stars, they have not retained their chemical peculiarity. Most of them have probably never been Am in the past.
- One-third of the metallic F0-6 giants are fast rotators with $v \sin i > 100$ km s^{-1}, while practically all Am stars are slow rotators with $v \sin i < 100$ km s^{-1}. Moreover, the shape of the $v \sin i$ distribution is completely different in each case: for metallic F0-6III stars it is flat with a cut-off at about 160 km s^{-1}, while that of Am stars shows a maximum between 30 and 40 km s^{-1} with a steady decrease towards 100 km s^{-1}. This still holds valid when the giant F sample is restricted to stars not known as δ Scuti type.
- The non-metallic giants have the same $v \sin i$ distribution as the metallic ones.
- The rate of binaries among normal A-F giants is no more than 47% for orbital periods less than 1000 days. This fraction may be overestimated because part of the V_r variations observed might be due to δ Scuti-type variations rather than orbital motion.
- For metallic F giants (considering or not δ Scuti stars), the best data in the literature together with our measurements indicate a rate of binaries with $P < 1000$ days of less than 30%. This is smaller, though not significantly so, than for normal giants. We may have missed binaries with a fast rotating primary, since the best V_r data in the literature concern sharp-lines stars (hence slow rotators). However, one sees no reason why most binaries should be in this case, especially as tidal friction would tend to slow down axial rotation. For Am stars, this rate is 75% (Abt & Levy 1985).

It seems therefore difficult to admit that Am stars can be progenitors of metallic F giants. If such was the case, one should indeed expect:

1. A larger rate of binaries among metallic giants than among normal ones, its value being close to that of Am stars (75%)
2. A $v \sin i$ distribution of metallic giants strongly peaked at very small values, with a tail extending to less than 100 km s^{-1}. Indeed, the giants are all about to leave the main sequence and have, on average, larger radii than Am stars. Therefore they can only rotate more slowly, by conservation of angular momentum.
3. Widely different $v \sin i$ distributions for the normal, than for the metallic giants, as is the case for the normal A dwarfs compared with the Am stars.

None of these three expectations is fulfilled. As a whole, the metallic giants cannot be considered as evolved Am stars, although the previous considerations do not exclude the possibility that some of them (especially the slower rotators) may have been Am stars in the past.

One might object that even fast rotating metallic giants may have main sequence metallic progenitors, but the latter have gone unnoticed by the classifiers because of fast rotation. But such progenitors would have been detected by Geneva or Strömgren photometry (through the m_2 or m_1 parameters), while significant photometric metallicity is observed only in stars classified spectroscopically as Am, except for the metallic F giants. The assumption of overabundances remaining steady (apart from that of Ca) up to the very end of the main sequence life therefore seems wrong, and diffusion theory indeed predicts that they may change drastically on shorter timescales, at least near the ZAMS (Alecian 1996).

But if metallic F giants are not evolved Am stars, what is their origin then? The fact that they are not especially slow rotators is intriguing, because it suggests that no special initial conditions are required to produce them. The

same can be said about the rate of binaries, which does not seem special either. In view of this, the very simplest alternative to the idea of Am progenitors is to speculate that every late A and early F star goes through a short phase of enhanced atmospheric metallicity around the end of its life on the main sequence.

We have seen that for some FIII stars the metallicity can coexist with high projected rotational velocity ($\geq$ 100 km s^{-1}). The explanation of this fact is a real challenge addressed to theoreticians of diffusion, because for main sequence stars metallicity can appear only in slow rotators ($\leq$ 100 km s^{-1}).

Acknowledgements. This research has made use of the Simbad database, operated at CDS, Strasbourg, France. We thank Drs. Michel Mayor and Stéphane Udry (Geneva Observatory) for providing us Coravel data for standard stars. We thank Mrs B. Wilhelm for the correction of the English text. This paper received the support of the Swiss National Science Foundation.

Appendix

Importance of the choice of the limits for the fit of the Hβ line

Simulations were carried out to observe the behaviour of $\overline{\lambda_0(\mathrm{H}\beta)}$ and $\sigma_{\lambda_0(\mathrm{H}\beta)}$ as a function of the choice of the two segments in order to find their optimal position and length.

Synthetic spectra were computed at 6000 K and 7500 K with a log$g$ of 4 and solar metallicity. They were then convoluted by instrumental and rotational profiles. We considered projected rotational velocities of 50 and 100 km s^{-1}. Finally, a random noise was added, corresponding to a signal-to-noise ratio of 150.

Two types of simulations were performed:

1. Two internal limits of the segments were fixed symmetrically with respect to the centre of the line, the external limits being moved away progressively from the line's centre. $\overline{\lambda_0(\mathrm{H}\beta)}$ and $\sigma_{\lambda_0(\mathrm{H}\beta)}$ was then computed for each position of these segments.
2. The external limits of the segments were fixed, the internal limits being brought regularly towards the centre of the line and $\overline{\lambda_0(\mathrm{H}\beta)}$ and $\sigma_{\lambda_0(\mathrm{H}\beta)}$ were again computed.

The results are given in Figs. 12 and 13, the upper part of them showing the variation of $\sigma_{\lambda_0(\mathrm{H}\beta)}$ and the lower part the variation of $\overline{\lambda_0(\mathrm{H}\beta)}$ as a function of the limits for the 4 spectra. Each curve corresponds to different initial conditions, i.e. to different fixed limits. The first type of simulation is represented by dotted lines and the second type by dots and dashes. The dispersion and the mean central wavelength are given as a function of the moving limit. To make these graphics easier to read, we have represented the right wing of the Hβ line with the scale in normalised flux (right axis of the graphics).

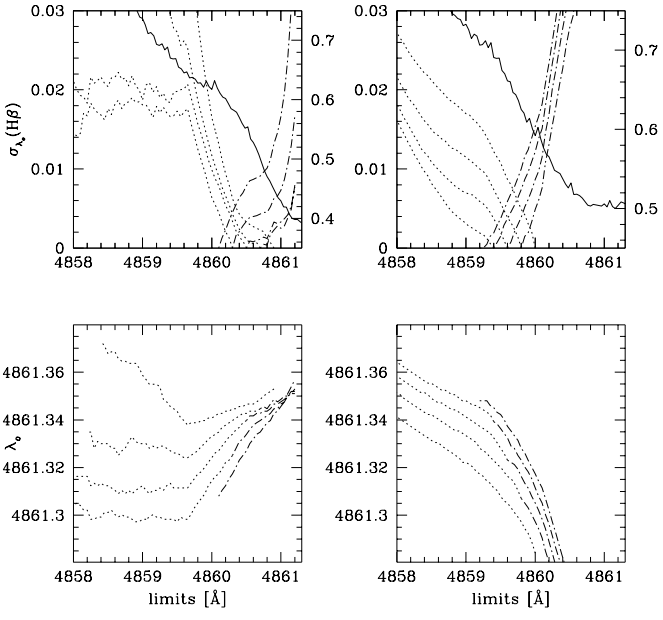

Fig. 12. Variation of $\overline{\lambda_0(\mathrm{H}\beta)}$ and $\sigma_{\lambda_0(\mathrm{H}\beta)}$ as a function of the limits for a star of 6000 K with a log$g$ of 4 and a solar metallicity. The graph at the left simulates variations for a $v \sin i$ of 50 km s^{-1} and at the right of 100 km s^{-1}. See text for comments

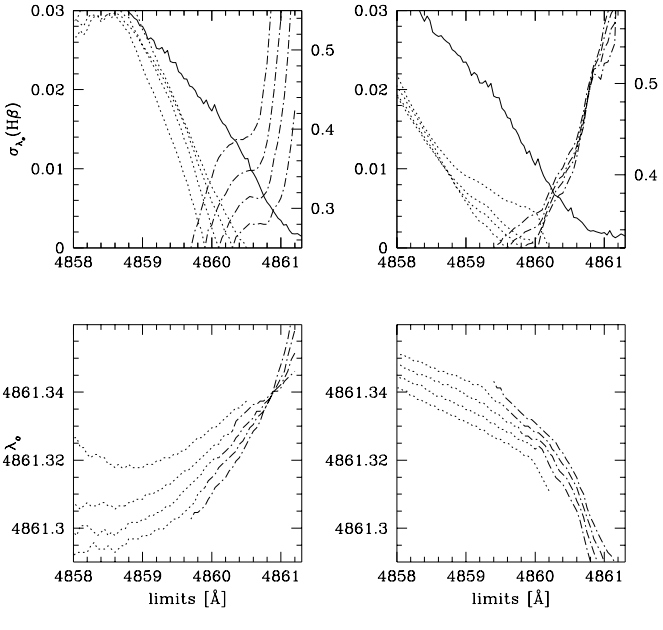

Fig. 13. Same as Fig. 11, but with $T_{\mathrm{eff}} = 7500$ K

First, let us discuss the behaviour of $\sigma_{\lambda_0(\mathrm{H}\beta)}$. When the internal and external limits are the same on each wing, the dispersion is evidently null, increasing when the internal and external limits are separated. This increase depends on each profile as seen in Figs. 12 and 13. Nevertheless, we can make general remarks. First, the nearer the limits to the centre of the line, the stronger the dispersion. This is easily understood, because near the centre only a few points are taken into account to make the fit and a weak change of limits leads to important changes of the three parameters of $L(\lambda)$. These parameters are not well defined either when we choose external limits too far from the centre, because Hβ have a lorentz profile only near the centre. Thus limits that are neither too close nor too far from the centre have to be chosen. Generally speaking, these subjective criteria are satisfactory when the segments lie on the linear part of the Hβ profile.

Increased $v \sin i$ and T_{eff} make the determination of the central wavelength more difficult because the line is wider. The dispersion therefore increases with $v \sin i$ and T_{eff}. When the segments are on the linear part of the profile, the following dispersions result: at 6000 K, $\sigma_{\lambda_0(\mathrm{H}\beta)}$ varies from 0.003 to 0.007 Å for $v \sin i$ equal to 50 and 100 km s^{-1} respectively and at 7500 K, its values are 0.004 to 0.007 Å for the same $v \sin i$. Thus the dispersion mainly depends on the rotational velocity and barely on the effective temperature.

On the lower graphics, one sees that $\overline{\lambda_0(\mathrm{H}\beta)}$ varies much as a function of the position and lengths of the segments. Nevertheless, if we consider only the linear portion, the variability of this parameter is not so important and corresponds to values given above. We observe that the shape of these fluctuations depends essentially on the $v \sin i$: for a $v \sin i$ of 100 km s^{-1}, $\overline{\lambda_0(\mathrm{H}\beta)}$ regularly decreases when the limits approach the centre of the line; for a $v \sin i$ of 50 km s^{-1} we observe an opposite trend.

The results of these simulations give only a qualitative idea about the behaviour of $\overline{\lambda_0(\mathrm{H}\beta)}$ and $\sigma_{\lambda_0(\mathrm{H}\beta)}$ as a function of the chosen segments. We have shown that these parameters are very sensitive to the limits, which have to be put on the linear parts of the line profile to alleviate this problem. For a given star, we always use the same limits in order to have a good internal coherence. Nevertheless, we may have systematic errors, but this is not a severe problem because we are interested in variations of radial velocity rather than in absolute values.

References

Abt H.A., 1965, ApJS 11, 429
Abt H.A., 1969, ApJS 19, 387
Abt H.A., Biggs E.S., 1972, Bibliography of Stellar Radial Velocities, Latham Process Corp., New York
Abt H.A., Levy S.G., 1976, ApJS 30, 273
Abt H.A., Levy S.G., 1985, ApJS 59, 229
Abt H.A., Morrell N.I., 1995, ApJS 99, 135
Abt H.A., Moyd K.I., 1973, ApJ 182, 809
Adams W.S., 1923, ApJ 57, 149
Adams W.S., Joy A.H., Sanford R.F., Strömberg G., 1929, ApJ 70, 207
Alecian G., 1996, A&A 310, 878
Baranne A., Mayor M., Poncet J.-L., 1979, Vistas Astron. 23, 279
Bernacca P.L., Perinotto M., 1971, Contr. Oss. Astrofis. Univ. Padova 249
Berthet S., 1990, A&A 227, 156
Berthet S., 1991, A&A 251, 171
Berthet S., 1992, A&A 253, 451
Boyarchuk A.A., Kopylov I.M., 1964, Publ. Obs. Crimee, 31, 44
Breger M., 1979, PASP 91, 5
Buscombe W., Morris P.M., 1958, MNRAS 118, 609
Campbell W.W., 1911, Lick Obs. Bull. 6, 140
Campbell W.W., 1912, Lick Obs. Bull. 7, 19
Campbell W.W., 1913, Lick Obs. Bull. 7, 113
Campbell W.W., 1928, Pub. of the Lick Obs. 16, 1
Cannon J.B., 1920, Pub. Dominion Obs. 4, 253
Catchpole R.M., Evans D.S., Jones D.H.P., King D.L., Wallis R.E., 1982, Royal Greenwich Obs. Bull. 188, 5
Charbonneau P., Michaud G., 1991, ApJ 370, 693
Cochran W.D., Hatzes A.P., Hancock T.J., 1991, ApJ 380, 35
Cowley A.P., 1976, PASP 88, 95
Cowley A.P., Cowley C.R., Jaschek M., Jaschek C., 1969, AJ 74, 375
Curchod A., Hauck B., 1979, A&AS 38, 449
Duquennoy A., Mayor M., 1991, A&A 248, 485
Evans D.E., Menzies A., Stoy R.H., 1957, MNRAS 117, 534
Evans D.E., Menzies A., Stoy R.H.,Wayman P.A., 1961, Royal Greenwich Obs. Bull. 48, 389
Evans D.E., Laing J.D., Menzies A., Stoy R.H., 1964, Royal Greenwich Obs. Bull. 85, 207
Evans D.E., 1966, Royal Greenwich Obs. Bull. 110, 185
Frost E.B., Barrett S.B., Struve O., 1929, Pub. Yerkes Obs. 7, 1
Gillet D., Burnage R., Kohler D., et al., 1994, A&AS 108, 181
Harper W.E., 1920, Pub. Dominion Obs. 4 , 331
Harper W.E., 1934, Pub. Dominion Astrophys. Obs. 6, 151
Harper W.E., 1937, Pub. Dominion Astrophys. Obs. 7, 1
Hauck B., 1973, problems of calibration of Absolute Magnitudes and Temperature of Stars, IAU Symp. 54, 117
Hauck B., 1986, A&A 155, 371
Hauck B., Curchod A., 1980, A&A 92, 289
Hauck B., Jaschek C., Jaschek M, Andrillat Y., 1991, A&A 252, 260
Henroteau F., 1923, Pub. Dominion Obs. 8, 59
Hoffleit D., Jaschek C., 1982, The Bright Star Catalogue, 4th revised edition, Yale University Observatory, New Haven
Houk N., Cowley A.P., 1975, Michigan Catalogue of Two-Dimensional Spectral Types for the HD Stars, Univ. of Michigan, Ann Arbor, Vol. 1
Houk N., 1978, Michigan Catalogue of Two-Dimensional Spectral Types for the HD Stars, Univ. of Michigan, Ann Arbor, Vol. 2
Houk N., 1982, Michigan Catalogue of Two-Dimensional Spectral Types for the HD Stars, Univ. of Michigan, Ann Arbor, Vol. 3
Jaschek M., 1978, A Catalogue of Selected MK Types, Inf. Bull. CDS 15, 121

Jones H.P., Haslam C.M., 1969, Royal Greenwich Obs. Bull., 155
Jordan F.C., 1912, Pub. Allegheny Obs. 2, 121
Künzli M., North P., Kurucz R.L., Nicolet B., 1996, A&AS 122, 51
Kurtz D.W., 1976, ApJS 32, 651
Latham D.W., Mazeh T., Stefanik R.P., Mayor M., Burki G., 1989, Nat 339, 38
Mayor M., Maurice E., 1985, in: Stellar radial velocities, IAU Coll. No. 88, eds. A.G. Davis Philip and David W. Latham. Davis Press, p. 299
Mayor M., Mazeh T., 1987, A&A 171, 157
Mayor M., Udry S., 1996 (private communication)
Mazeh T., Goldberg D., Duquennoy A., Mayor M., 1992, ApJ 401, 265
Michaud G., Charland Y., Vauclair S., Vauclair G., 1976, ApJ 210, 447
Michaud G., Tarasick D., Charland Y., Pelletier C., 1983, ApJ 269, 239
Nelson J.N., Kreidl T.J., 1993, AJ 105, 1903
Neubauer F.J., 1930, Lick Obs. Bull. 15, 46
Nordström B., Andersen J., 1985, A&AS 61, 53
North P., 1994, in: The 25th workshop and meeting of European working group on CP stars, Jankovics I. and Vincze I.J. (eds.), Gothard Astrophysical Observatory of Eötvös University, Szombathely, Hungary, p. 3
0'Brien G.T., et al., 1986, ApJS 62, 899
Penfold J.E., 1971, PASP 83, 497
Plaskett W.E., Harper W.E., Young R.K., Plaskett H.H., 1921, Pub. Dominion Astrophys. Obs., 2, 1. Spencer Jones, H., 1928, CAPE 10-8, 95
Rodriguez E., Lopez de Coca P., Rolland A., Garrido R., Costa V., 1994, A&AS 106, 21
Rosvick J.M., Scarfe C.D., 1991, PASP 103, 628
Sanford R.F., Karr E., 1942, ApJ 96, 214
Shajn G., Albitzky V., 1932, MNRAS 92, 771
Smith M.A., 1982, ApJ 254, 242
Tassoul J.-L., Tassoul M., 1992, ApJ 395, 259
Uesugi A., Fukuda I., 1978, Preliminary Catalogue of Rotational velocities, CDS
Uesugi A., Fukuda I., 1982, Revised Catalogue of Rotational Velocities, Uni. of Kyoto
Vauclair S., Vauclair G., 1982, ARA&A 20, 37
Wilson R.E., Joy A.H., 1950, ApJ 111, 221
Wooley R., Penston M.J., Harding G.A., Martin W.L., Sinclair C.M., Aslan S., Savage A., Aly K., Assad A.S., 1971, Royal Greenwich Obs. Ann. 14, 1
Zahn J.P., 1977, A&A 57, 383